Dynamics of the vacuolar H+-ATPase in the contractile vacuole complex and the endosomal pathway of *Dictyostelium* cells

Margaret Clarke[1],*, Jana Köhler[2], Quyen Arana[1], Tongyao Liu[1], John Heuser[3] and Günther Gerisch[2]

[1]Oklahoma Medical Research Foundation, Oklahoma City, Oklahoma, USA
[2]Max-Planck-Institut für Biochemie, D82152 Martinsried, Germany
[3]Washington University School of Medicine, St Louis, Missouri, USA
*Author for correspondence (e-mail: clarkem@omrf.ouhsc.edu)

Summary

The vacuolar H+-ATPase (V-ATPase) is a multi-subunit enzyme that plays important roles in eukaryotic cells. In *Dictyostelium,* it is found primarily in membranes of the contractile vacuole complex, where it energizes fluid accumulation by this osmoregulatory organelle and also in membranes of endolysosomes, where it serves to acidify the endosomal lumen. In the present study, a fusion was created between *vatM*, the gene encoding the 100 kDa transmembrane subunit of the V-ATPase, and the gene encoding Green Fluorescent Protein (GFP). When expressed in *Dictyostelium* cells, this fusion protein, VatM-GFP, was correctly targeted to contractile vacuole and endolysosomal membranes and was competent to direct assembly of the V-ATPase enzyme complex. Protease treatment of isolated endosomes indicated that the GFP moiety, located on the C-terminus of VatM, was exposed to the cytoplasmic side of the endosomal membrane rather than to the lumenal side. VatM-GFP labeling of the contractile vacuole complex revealed clearly the dynamics of this pleiomorphic vesiculotubular organelle. VatM-GFP labeling of endosomes allowed direct visualization of the trafficking of vacuolar proton pumps in this pathway, which appeared to be entirely independent from the contractile vacuole membrane system. In cells whose endosomes were pre-labeled with TRITC-dextran and then fed yeast particles, VatM-GFP was delivered to newly formed yeast phagosomes with the same time course as TRITC-dextran, consistent with transfer via a direct fusion of endosomes with phagosomes. Several minutes were required before the intensity of the VatM-GFP labeling of new phagosomes reached the level observed in older phagosomes, suggesting that this fusion process was progressive and continuous. VatM-GFP was retrieved from the phagosome membrane prior to exocytosis of the indigestible remnants of the yeast particle. These data suggest that vacuolar proton pumps are recycled by fusion of advanced with newly formed endosomes.

Movies available on-line

Key words: *Dictyostelium*, V-ATPase, Contractile vacuole, Endosome, Phagosome, GFP

Introduction

All eukaryotic cells contain a highly conserved multi-subunit enzyme, the vacuolar H+-ATPase or V-ATPase, which uses the energy from ATP hydrolysis to transport protons across biological membranes (reviewed by Nelson and Harvey, 1999; Wieczorek et al., 1999; Forgac, 2000). The protons may serve to acidify an intracellular compartment or an extracellular space, or the proton gradient may energize the transport of other ions or macromolecules. The action of the multi-subunit V-ATPase complex is regulated at several levels. Distinct isoforms of the enzyme may be localized to different compartments within a single cell (Manolson et al., 1992; Manolson et al., 1994) or to different cell types in a multicellular organism (Nishi and Forgac, 2000; Mattsson et al., 2000; Oka et al., 2001). The distribution and/or activity of the enzyme may also be altered in response to environmental or developmental cues (Sumner et al., 1995; Kane, 1995; Wieczorek et al., 1999).

The V-ATPase consists of two functional subcomplexes, V_1 and V_0. V_1 is a peripheral complex of at least eight subunits that is responsible for ATP hydrolysis. V_0 is an integral membrane complex of at least five subunits that carries protons across the membrane. Mutational analysis of Vph1p, a *S. cerevisiae* isoform of the large (~100 kDa) transmembrane subunit of the V_0 complex, has shown that this protein is important in V-ATPase assembly and proton translocation (Leng et al., 1996; Leng et al., 1998). The role of the 100 kDa subunit in proton translocation has led to the suggestion that it is functionally similar to the 30 kDa 'a' subunit of the evolutionarily related F-ATPase, in spite of the difference in primary structure (Leng et al., 1996). The F-ATPase or ATP synthase of bacteria, mitochondria and chloroplasts is a rotary motor (Cross and Duncan, 1996; Junge et al., 1996; Noji et al., 1997), with intersubunit rotation leading to energy transduction. In the V-ATPase, which is thought to operate in a similar manner, Vph1p provides a link between the V_0 and V_1 sectors and thus may serve as a stator for the rotary motor (Landolt-Marticorena et al., 1999; Landolt-Marticorena et al., 2000).

The predicted amino acid sequence of Vph1p (and its homologues in many organisms) contains multiple potential membrane-spanning domains; estimates range from six or seven (Manolson et al., 1992; Nelson and Harvey, 1999) to nine (Leng et al., 1999). The hydrophilic N-terminal domain of Vph1p has been shown to face the cytosolic side of the membrane (Jackson and Stevens, 1997; Landolt-Marticorena, 1999), but the orientation of the C-terminal domain is not known with certainty. Random mutagenesis of Vph1p identified certain amino acids between residues 800 and 814 (…LxWVxxxxxFxxxxG…) that, when mutated, led to a substantial decrease in the assembly of the V-ATPase complex; mutations of the F and G residues also appeared to affect targeting of this subunit (Leng et al., 1998). All of these residues lay beyond the last presumptive transmembrane domain of the protein, near the C-terminus. The finding that the C-terminus of Vph1p is important for enzyme assembly suggested that the C-terminus extended into the cytoplasm, where it could associate with the V_1 sector (Leng et al., 1998). However, a subsequent study from the same laboratory employing cysteine scanning mutagenesis and labeling by sulfhydryl reagents of differing membrane permeabilities led to the opposite conclusion, namely, that the C-terminus of Vph1 probably resides in the vacuole lumen (Leng et al., 1999). In the latter model, (lumenal) amino acids 800-814 were postulated to regulate protein conformation in cytoplasmic as well as lumenal domains of the protein (Leng et al., 1999).

The eukaryotic microorganism *Dictyostelium discoideum* appears to contain a single isoform of the V-ATPase 100 kDa subunit (VatM), as determined by PCR-based assays (Liu and Clarke, 1996) and indicated by the largely completed sequence of the *Dictyostelium* genome. VatM is 40% identical to Vpp1, the rat clathrin-coated vesicle/synaptic vesicle 116 kDa V-ATPase subunit and is 37% identical to Vph1p of *S. cerevisiae*. In *Dictyostelium*, VatM has been localized to the membranes of two compartments, the contractile vacuole complex (Fok et al., 1993), an osmoregulatory organelle in which the proton pumps energize water movement from the cytosol into the vacuole complex (Heuser et al., 1993), and the endolysosomal system (Adessi et al., 1995), in which the proton pumps serve to acidify the lumen of endosomes. These compartments are physically distinct (Gabriel et al., 1999), although mutations have been identified that affect both organelles (O'Halloran and Anderson, 1992; Ruscetti et al., 1994; Bush et al., 1996), suggesting that a membrane trafficking relationship exists between them. There is a substantial difference in the abundance of proton pumps in the membranes of these two organelles; the pump density in contractile vacuole membranes is greater by a factor of about ten (Rodriguez-Paris et al., 1993; Clarke and Heuser, 1997).

We have created a fusion of VatM to green fluorescent protein (GFP) in order to monitor the activity of the contractile vacuole complex and the trafficking of the V-ATPase in the endocytic pathway of living *Dictyostelium* cells. The fusion protein, VatM-GFP, is correctly targeted to contractile vacuole and endosomal membranes. This fluorescent V-ATPase subunit has enabled us to visualize the distribution of proton pumps in the contractile vacuole system during the interconversion of vacuolar and tubular elements as this organelle takes up and expels fluid. VatM-GFP has also permitted real-time visualization of the trafficking of proton pumps to phagosomes. This marker has revealed that the principal route of delivery of the V-ATPase to phagosomes is as a component of the membrane of pre-existing acidic endosomal vesicles.

Materials and Methods

Cells and growth conditions

The cells used in this study were *Dictyostelium discoideum* 'wild-type' strains AX2 and AX3, and VatMpr, a conditional VatM mutant (Liu et al., 2002). *Dictyostelium* cells were cultivated at 21°C in HL5 (Clarke et al., 1980). Cells were also grown in association with *Klebsiella aerogenes* either on SM agar plates (Loomis, 1975) or in a suspension of bacteria harvested from such plates in phosphate buffer (17 mM Na_2H/KH_2PO_4 buffer, pH 6.0), as described previously (Rathi et al., 1991). *S. cerevisiae* strain TH2-1B (a gift of W. Tanner, Regensburg, Germany) was cultivated in YPD (Rose et al., 1990) at 30°C.

Preparation and expression of a VatM-GFP fusion protein

A GFP gene containing the S65T mutation was recovered by PCR from the plasmid pRSET using DeepVent polymerase (New England Biolabs). The forward primer was 5′-CC<u>CTGCAG</u>(GGTGCA)₅AT-GAGTAAAGGAGAAGAACTT-3′, which added a *Pst*I site (underlined) and five tandem (gly ala) codons to the 5′-end of the *GFP* gene; the reverse primer was 5′-TCTAGAGTTATTGCTCA-GCGGTGG-3′ (pRSET Reverse, Invitrogen). The PCR product was cut with *Bam*HI (which cut at a site in the pRSET polylinker immediately adjacent to the 3′ end of the GFP gene) and cloned into pBluescript-SK⁻ cut with *Eco*RV and *Bam*HI. The resulting plasmid, pSK⁻/(GA)₅-GFP, was cut with *Pst*I and *Sal*I, and the large fragment containing the *GFP* gene plus the vector was isolated. The plasmid pVM1 (Liu and Clarke, 1996) was used as a template to generate the VatM coding sequence by PCR, again using DeepVent polymerase. The primers were 5′-CC<u>GAGCTC</u>ATGAGCTTTTTAAGACCATCC-3′ (forward) and 5′-CC<u>CTGCAG</u>TTCATC TTCAGAAAGAATAC-3′ (reverse), which added *Sac*I and *Pst*I restriction sites at the 5′ and 3′ ends of the *vatM* gene, respectively. The PCR product was cloned into pBluescript-SK⁻ at its *Eco*RV site, and the resulting plasmid was cut with *Pst*I and *Sal*I, releasing the VatM coding sequence. This was inserted into pSK⁻/(GA)₅-GFP cut with the same two enzymes (as described above), yielding an in-frame fusion of the VatM coding sequence with that for (gly ala)₅-GFP, the GFP being positioned at the C-terminus of the fusion protein. (The C-terminus of VatM normally ends …SEDDE*; the fusion junction is …SEDEQQ(GA)₅….) The restriction fragment encoding VatM-GFP was excised with *Sac*I and *Xba*I and cloned into the *Dictyostelium* expression vector pDXA-3H (Manstein et al., 1995) cut with the same two enzymes, yielding pDXA/VatM-GFP.

AX3-ORF⁺ cells (Manstein et al., 1995) growing in HL5 were harvested at a density of 1×10^6 cells/ml, pelleted by centrifugation and suspended in electroporation buffer (8.75 mM NaH_2PO_4, 1.25 mM Na_2HPO_4, 2 mM sucrose) at 1×10^7 cells/ml. One ml of cells was mixed with 20 μg of the pDXA/VatM-GFP plasmid. The cells were electroporated using a BioRad Gene Pulser at 1.6 kV/cm. Cells were then transferred to 10 cm tissue culture plates and left overnight in HL5. The next day G418 was added to a final concentration of 5 μg/ml. The cells were diluted 10-fold and plated in 96-well tissue culture plates for clonal selection. Transformation of VatMpr cells was carried out as above except that 20 μg pREP (Manstein et al., 1995) was co-transfected with pDXA/VatM-GFP. (pREP contains the Ddp2 ORF sequence necessary for pDXA replication in strains other than AX3-ORF⁺, which carries this sequence on the chromosome.) Transformants were screened by epifluorescence microscopy to identify clones with bright GFP labeling of intracellular membranes.
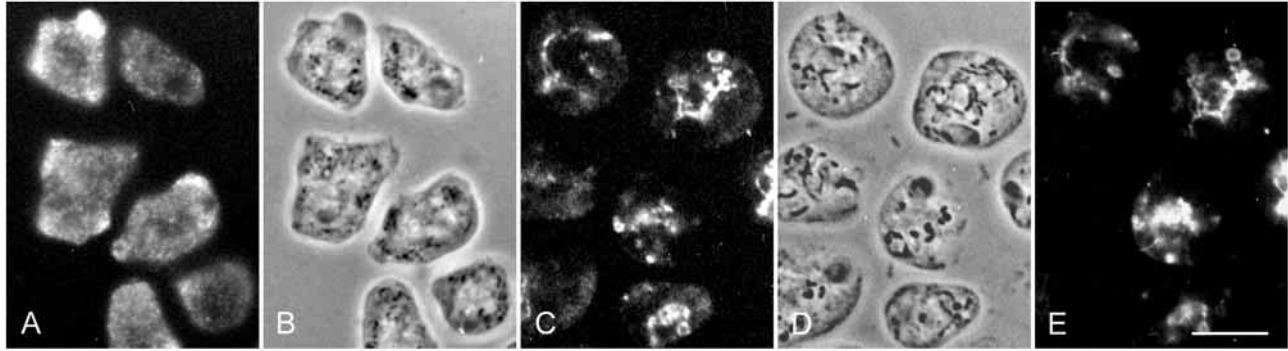
Fig. 1. Effect of VatM-GFP expression on the distribution of VatA in bacterially grown VatMpr cells. VatMpr and VatMpr/VatM-GFP cells were grown for two days on *K. aerogenes*, then fixed and stained with the N4 monoclonal antibody, which recognizes the A subunit of the V-ATPase, followed by Cy3-labeled anti-mouse antibodies. A and B show VatMpr cells (A, Cy3; B, phase contrast), and C to E show VatMpr/VatM-GFP cells (C, Cy3; D, phase contrast; E, GFP). VatA is diffusely distributed in VatMpr cells (A), but, as seen in C, colocalizes with VatM (E) on contractile vacuole membranes in VatMpr/VatM-GFP cells. In cells with poor expression of VatM-GFP, VatA remains diffuse (two cells at the lower left in C and E). Bar, 10 μm.

Indirect immunofluorescence methods

D. discoideum cells (VatMpr and VatMpr/VatM-GFP) were grown in suspension in association with *K. aerogenes* for two or three days before being examined. Samples were taken from low-density, exponentially growing cultures and washed free of bacteria by three cycles of centrifugation in 17 mM Na/KPO$_4$ buffer (pH 6.4). After agar-overlay, the cells were fixed in the same buffer containing 2% formaldehyde (5 minutes, room temperature), followed by 1% formaldehyde in methanol (5 minutes, –15°C). The cells were stained with N4 hybridoma culture supernatant (diluted 1:20), which labels the V-ATPase A subunit (Fok et al., 1993), followed by Cy3-conjugated donkey anti-mouse IgG (1:500, Jackson ImmunoResearch Laboratories). A detailed description of the staining methods may be found in Clarke et al. (Clarke et al., 1987).

Fluorescence microscopy of living cells

Cells from axenic culture were plated on a glass coverslip (5×5 cm) within a plastic ring 40 mm in diameter. After the cells had settled and attached, the axenic medium was replaced with 17 mM Na/KPO$_4$ buffer (pH 6.0) or with fresh nutrient medium diluted 3- to 10-fold in this buffer, as indicated. For labeling of the endosomal compartment, cells were incubated in dilute axenic medium containing 2 mg/ml tetramethylrhodamine isothiocyanate (TRITC)-dextran (Sigma, M_r 70,000) for 30 to 90 minutes. In some experiments, cells were observed in this medium; in others, it was replaced with phosphate buffer prior to observation of the cells. For monitoring phagocytosis, a suspension of living yeast cells in phosphate buffer was added to the *Dictyostelium* cells. Just prior to observation, the *Dictyostelium* cells were compressed under a thin layer of agarose prepared as described by Yumura et al. (Yumura et al., 1984). In some experiments, the agarose layer had first been soaked in Neutral Red (2.5 μM in phosphate buffer) in order to label acidic compartments.

For all endocytosis and phagocytosis experiments, a Zeiss LSM 410 microscope equipped with a 100× 1.3 N.A. Plan Neofluar objective was used to collect simultaneous phase contrast and confocal fluorescence images of the cells. For excitation of S65T-GFP, the 488 band of an argon-ion laser was used together with a 515-565 nm filter for emission. For simultaneous recording of GFP and Neutral Red or TRITC-dextran, the 488 nm laser band was used together with the 543 nm band of a He-Ne laser, and emission was split by the use of a 510-525 nm filter for GFP and a 570 nm high pass filter for the fluorescence of other dyes. Simultaneous fluorescence and interference reflection microscopy (IRM) images showing the dynamics of the contractile vacuole complex in living cells (Fig. 3) were obtained using a BioRad Radiance 2000-AGR3 confocal microscope equipped with a Zeiss 100×, 1.4 N.A. planapochromat objective lens.

Purification of TRITC-dextran-loaded endosomes from *Dictyostelium* cells

D. discoideum cells expressing VatM-GFP were cultivated in association with *K. aerogenes* on SM agar plates and harvested prior to clearing of the bacterial lawn. The cells were suspended at 5×10^6 cells/ml in AX2 medium containing 0.2 mg/ml TRITC-Dextran (Sigma, 70,000 M_r) and incubated on a rotary shaker at 22°C for 6 hours. The cells were harvested by sedimentation, washed once in cold phosphate buffer and once in cold homogenization buffer (50 mM Tris-HCl, pH 7.6, 25 mM KCl, 5 mM MgCl$_2$, 100 mM sucrose), then suspended in 1.5 ml of the same buffer. The cell suspension was placed in a syringe and forced twice through a stack of two polycarbonate filters (Nucleopore, 5 μm pore size). The cell lysate was centrifuged at 500 g for 10 minutes at 4°C to remove unbroken cells. The supernatant was loaded on a Percoll gradient (2.5 ml each of 70%, 65% and 60% Percoll in homogenization buffer) and spun for 1 hour at 80,000 g. A faintly visible band was recovered from the middle of the gradient. Epifluorescence microscopy confirmed that TRITC-dextran-containing vesicles were present in this fraction.

Results

Construction and biological activity of VatM-GFP

A construct was prepared as described in Materials and Methods that expressed the complete sequence of VatM fused at its C-terminus to a flexible linker followed by GFP containing the S65T mutation. Wild-type *Dictyostelium* cells and the mutant VatMpr were transformed with this construct. VatMpr is a strain in which the chromosomal *vatM* promoter has been replaced by the *act6* promoter, resulting in reduced expression of *vatM* when cells are grown on bacteria (Liu et al., 2002). In both cell types, VatM-GFP was correctly targeted to membranes of the contractile vacuole complex and the endolysosomal system, as shown in subsequent sections of this report.

VatMpr cells were used to assess the biological activity of VatM-GFP. These cells contain approximately normal levels of

VatM (and vacuolar proton pumps) when they are grown axenically, but when they are cultured on bacteria, the level of VatM drops to about one-third of normal. This deficiency has several phenotypic consequences, including slow growth of the cells on bacteria and redistribution of VatA, the peripheral catalytic subunit of the V-ATPase, from membranes to the cytoplasm (Liu et al., 2002). We examined whether VatM-GFP expressed in VatMpr cells could correct these defects. Bacterially grown VatMpr and VatMpr/VatM-GFP cells were fixed and stained to visualize the distribution of VatA. Expression of VatM-GFP proved to be sufficient to correct the mislocalization of VatA (Fig. 1). In VatMpr/VatM-GFP cells, antibodies to VatA labeled contractile vacuole membranes (Fig. 1C), as they do in normal cells, colocalizing with VatM-GFP (Fig. 1E). This was in contrast to the diffuse cytoplasmic staining by anti-VatA observed in VatMpr cells not expressing VatM-GFP (Fig. 1A). These results demonstrate that VatM-GFP is correctly targeted to contractile vacuole membranes and that it is competent to direct assembly of the V-ATPase enzyme complex.

Nonetheless, VatM-GFP proved to be less effective than wild-type VatM in complementing certain other phenotypic defects of VatMpr cells. VatMpr/VatM-GFP cells continued to grow slowly on bacteria and were unable to complete development, defects characteristic of VatMpr cells (data not shown). Possibly, the presence of the GFP moiety on the C-terminus of VatM interferes to some degree with proton translocation, a key function of this subunit.

Orientation of C-terminal GFP on VatM

To examine the orientation of the C-terminus of VatM with its attached GFP moiety, we isolated endosomes from cells that had been fed TRITC-dextran, a fluorescent, membrane-impermeant fluid phase marker (see Materials and Methods for details). Cells were broken by the gentle technique of forcing them through 5 μm filters, and the cell lysate was fractionated on a Percoll gradient. Fractions were examined by epifluorescence microscopy using a rhodamine filter set, and the peak fraction of vesicles loaded with TRITC-dextran was identified (Fig. 2A). The membranes surrounding these vesicles were brightly labeled when viewed with the GFP filter set (Fig. 2B), confirming the presence of VatM-GFP in endolysosomal membranes.

Proteinase K (final concentration 100 μg/ml) was added to an aliquot of this vesicle fraction. After an incubation period of 7 minutes on ice, the vesicles were viewed by epifluorescence microscopy. The vesicles retained their TRITC-dextran fluorescence, indicating that the endosomal membranes had not been perforated (Fig. 2D). However, the GFP signal in the membranes of these vesicles had completely disappeared (Fig. 2E). The only remaining GFP fluorescence was in the membranes of a few tiny vesicles without red endosomal content, possibly fragments of membrane that had become resealed inside out during isolation. These results suggest that GFP, and thus the C-terminus of VatM, is exposed on the cytoplasmic rather than the lumenal side of the endosomal membrane.

VatM contains the same sequence of amino acids near its C-terminus (…LxWVxxxxxFxxxxG…) that were demonstrated by random mutagenesis to be important for association of the V_1 and V_0 domains in Vph1p (Leng et al., 1998). If, owing to
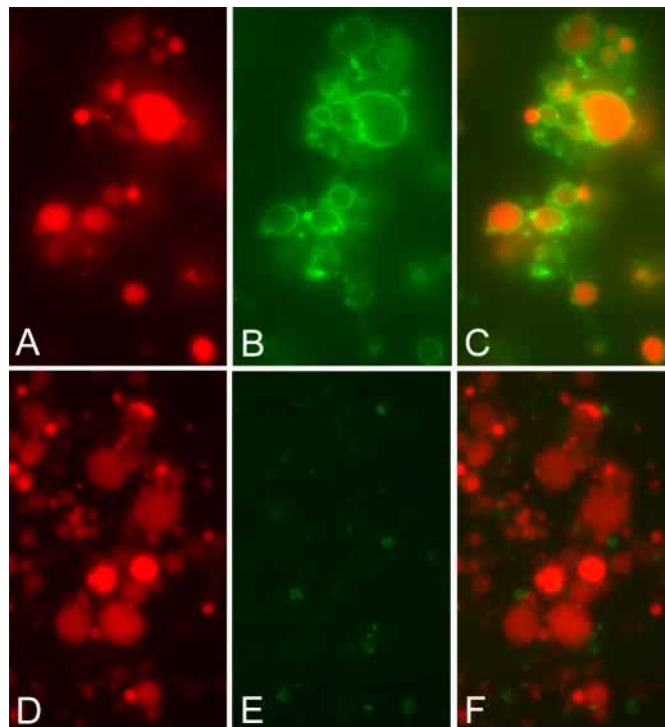

Fig. 2. Orientation of GFP on the C-terminus of VatM. Cells expressing VatM-GFP were fed TRITC-dextran, and endosomes were isolated on a Percoll gradient. Endosomes, identified by TRITC-dextran fluorescence (A), were rimmed with green fluorescence (B) from VatM-GFP in the endosomal membranes; C shows the two images overlaid. Following brief treatment with Proteinase K, TRITC-dextran was still present in the endosomes (D), although the green fluorescence (E) had disappeared from endosomal membranes; F shows the two images overlaid.

the attachment of the GFP moiety, the C-terminus of VatM were erroneously retained in the cytoplasm rather than being delivered to its proper location in the vacuole lumen, one would expect the improper location of these key residues to block the function of the C-terminal domain in enzyme targeting and assembly. However, VatM-GFP is quite functional in these respects, as described above. Thus, our results lend support to a model in which the C-terminus of the 100 kDa V-ATPase subunit resides in the cytoplasm.

Labeling of the contractile vacuole complex and endosomal membranes with VatM-GFP

In living *Dictyostelium* cells, the distribution of the fluorescent signal from VatM-GFP corresponded to that expected for vacuolar proton pumps on the basis of other methods of analysis (see Discussion). VatM-GFP strongly labeled membranes of the contractile vacuole complex (both the vacuolar and tubular elements) and, less strongly, endosomal membranes.

VatM-GFP provides an excellent marker for visualizing the dynamics of the contractile vacuole system. Fig. 3 and Movie 1 (available at jcs.biologists.org/supplemental) show the formation and discharge of multiple contractile vacuoles in an AX3/VatM-GFP cell. Using a confocal microscope, the cell
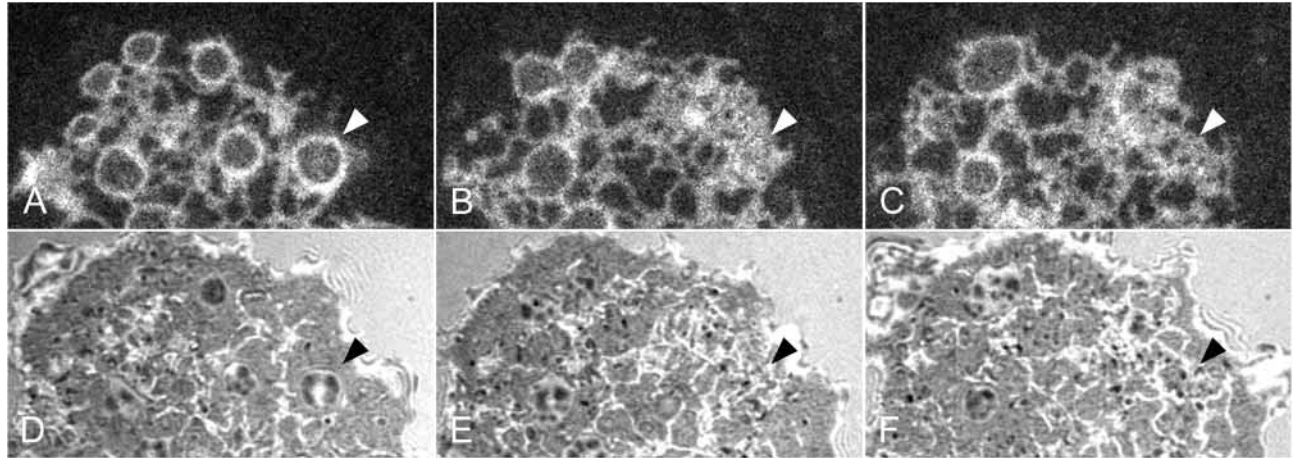
Fig. 3. Dynamics of the contractile vacuole system revealed by VatM-GFP and interference reflection microscopy. An AX3 cell expressing VatM-GFP was viewed simultaneously by fluorescence microscopy (A-C) and IRM (D-F). These images correspond to frames 14 (A,D), 36 (B,E) and 51 (C,F) from Movie 1. Images were captured at 1 second intervals, and so these images span a total of 36 seconds. Three vacuoles in the upper right portion of the cell emptied during this time interval and were replaced by a tracery of tubules. The arrowhead marks the same position in each frame. Two other vacuoles (upper left) fused during this same interval and later emptied (see Movie 1).
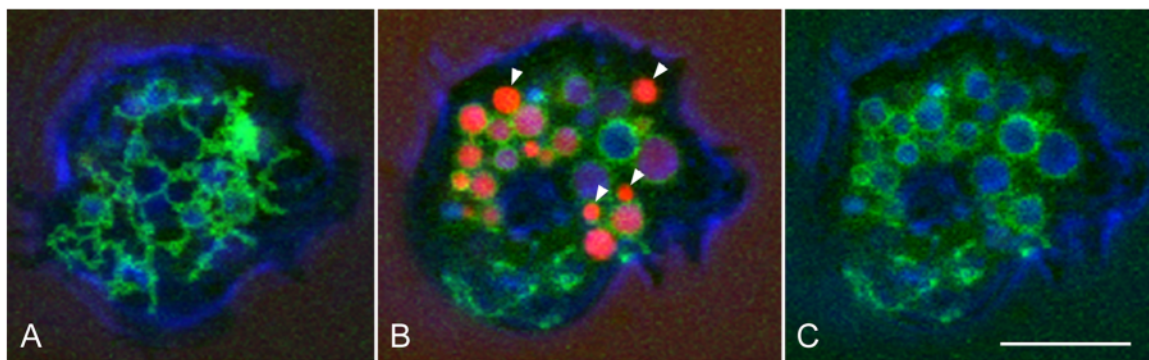

Fig. 4. Labeling of contractile vacuole and endosomal membranes with VatM-GFP. *Dictyostelium* cells expressing VatM-GFP were observed following a 70 minute incubation in one-third strength nutrient medium containing TRITC-dextran (2 mg/ml). Three signals were recorded: green (VatM-GFP), red (TRITC-dextran), and blue (phase contrast). All three channels are shown in A and B, whereas C shows the same image as B minus the red channel. A is a focal plane near the substratum showing the contractile vacuole complex, and B and C are a focal plane higher in the cell, showing several endosomes and also some elements of the contractile vacuole complex including several vacuoles, which are phase lucent. The arrows mark endosomes whose periphery is not labeled with VatM-GFP (presumptive late endosomes). Bar, 10 μm.

was viewed simultaneously by fluorescence and interference reflection microscopy (IRM). A time series was recorded for a single focal plane near the substratum, since this is the region of the cell where the contractile vacuole complex is primarily situated. The IRM and fluorescence views are shown separately for a portion of the cell in Fig. 3, so that the conversion of individual vacuoles to a network of tubules after emptying can be seen more clearly. The IRM and fluorescence views are overlaid in Movie 1. The highly dynamic and pleiomorphic nature of the contractile vacuole complex is evident, with continuous interconversion of vacuolar and tubular elements of the system as fluid is accumulated and expelled.

VatM-GFP also labels membranes of endolysosomes. The cell shown in Fig. 4 was incubated in nutrient medium containing TRITC-dextran for 70 minutes prior to observation. TRITC dextran is taken up by macropinocytosis, and, over this time interval, becomes distributed among vesicles at all stages of the endolysosomal pathway (Hacker et al., 1997; Jenne et al.,

1998). A focal plane near the substratum (Fig. 4A) displayed the contractile vacuole complex, whereas focal planes higher in the cell (e.g., Fig. 4B) were greatly enriched in endosomes filled with the red fluorescent fluid phase marker. The periphery of most of the endosomes was labeled with VatM-GFP, which is best seen after subtraction of the red channel (Fig. 4C). However, this cell, and others for which an hour or more had elapsed since first exposure to TRITC-dextran, also contained some endosomes not labeled with VatM-GFP (arrowheads). We presume these are late endosomes, from which vacuolar proton pumps have already been retrieved. Typically, the red fluorescence from such endosomes appeared more intense, indicating that the TRITC-dextran has become concentrated, as described previously (Maniak, 2001).

VatM-GFP in phagosomes

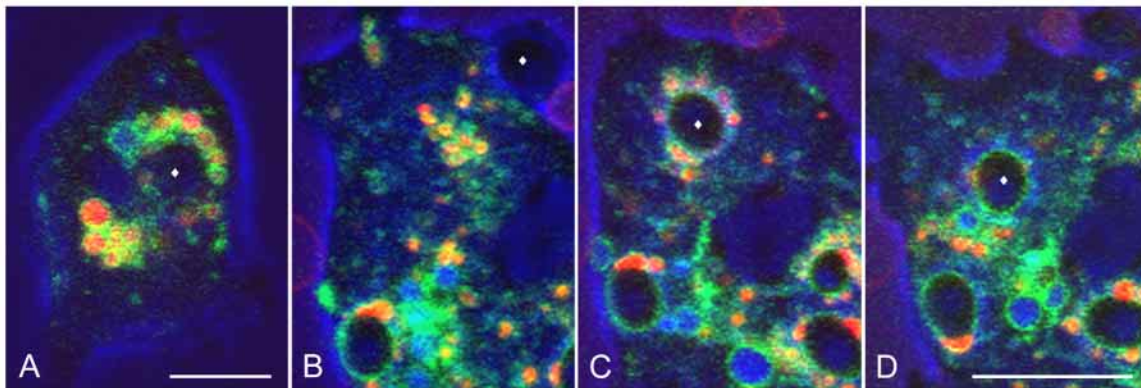*Dictyostelium* cells are avid phagocytes that consume not only

Fig. 5. Clustering of acidic endosomal vesicles labeled with VatM-GFP at the membrane of new phagosomes, followed by the appearance of VatM-GFP in the phagosome membrane. Cells expressing VatM-GFP were fed yeast particles in the presence of Neutral Red (A) or TRITC-dextran (B-D). The TRITC-dextran was present for at least 30 minutes before addition of the yeast. (A) Neutral Red-positive vesicles rimmed with VatM-GFP clustered next to a phagosome (2 minutes after uptake of the yeast particle). The yeast particle is marked with a white diamond. (B-D) A large cell containing several yeast particles taking up a new yeast particle (marked with a white diamond); (B) phagosome membrane closing around the new yeast particle; (C) clustering of TRITC-dextran-positive, VatM-GFP-rimmed vesicles at the membrane of the new phagosome (70 seconds later); (D) similar intensity of VatM-GFP label in membranes of new and old phagosomes (4 minutes after uptake). Bars, 10 μm.

bacteria, their natural prey, but also larger particles such as yeast cells, which are especially well suited for visualization by light microscopy. When cells expressing VatM-GFP are fed yeast particles, the appearance of GFP fluorescence in the phagosome membrane provides a marker for the delivery of vacuolar proton pumps to that membrane. Using this assay, we have monitored the delivery of proton pumps to phagosomes, their presence during the digestion of yeast particles and their disappearance from phagosome membranes prior to expulsion of the indigestible remnants of the particle.

VatM-GFP is delivered to the membrane of newly formed phagosomes in the membranes of small vesicles. These small vesicles begin clustering at the phagosome membrane about 1 to 2 minutes after uptake of the yeast particle. If the *Dictyostelium* cells are bathed in medium containing Neutral Red, a vital dye that passes through cell membranes and becomes trapped in acidic compartments, these small vesicles have red lumens, indicating that they are acidic (Fig. 5A). If, instead, the *Dictyostelium* cells are pre-incubated with TRITC-dextran, a membrane-impermeant fluid phase marker that enters cells by endocytosis, the content of the small GFP-rimmed vesicles is also red, demonstrating that they are endosomal vesicles (Fig. 5C). Within three or four minutes of particle uptake, TRITC-dextran from these endosomes can be

detected within the phagosome. Both Neutral Red and TRITC-dextran can sometimes be visualized as discrete patches under the phagosome membrane, presumably representing recent sites of vesicle fusion. Fig. 6A shows a cell labeled with Neutral Red, and Fig. 6B shows a cell labeled with TRITC-dextran; the latter cell had been washed free of TRITC-dextran before yeast particles were added. When the red channel is removed from the second image (Fig. 6C), it can be seen that the green VatM-GFP rim is continuous around the outer side of the mound of red marker, confirming that local fusion had occurred between the phagosome membrane and a vesicle filled with TRITC-dextran. Neutral Red labeled presumptive fusion sites along the phagosome membrane in a similar manner (Fig. 6A), indicating that the fusing vesicles were acidic. Thus, vacuolar proton pumps are delivered to phagosomes by pre-existing, acidic, endosomal vesicles, and the content of these vesicles is released into the phagosome.

Within the phagosome, endosomal fluid-phase markers accumulate predominantly at the necks of budded yeast cells, because the acute curvature at a bud neck precludes a snug fit of the phagosome membrane at this point, as previously described (Schneider et al., 2000). The yeast strain used here is partially impaired in cytokinesis, so most yeast particles have one or more buds. Localization of the marker in the
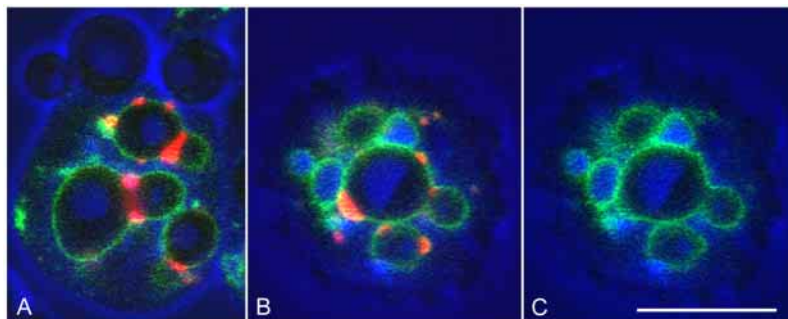
Fig. 6. Delivery of endosomal content to the phagosome. (A) A cell fed yeast in the presence of Neutral Red. Within the cell are three phagosomes containing yeast particles, all with Neutral Red accumulation at the bud neck. The upper phagosome also has mounds of Neutral-Red-positive material at sites along its membrane. (There are also two free yeast particles just above the cell; these are not stained.) (B,C) A cell whose endosomes were labeled with TRITC-dextran prior to addition of yeast particles. Mounds of TRITC-dextran are present along

the phagosome membrane (B). Subtraction of the red channel shows that VatM-GFP is continuous around the outside of these mounds (C), suggesting that they are sites of fusion between endosomal vesicles and the phagosome membrane. Bar, 10 μm.
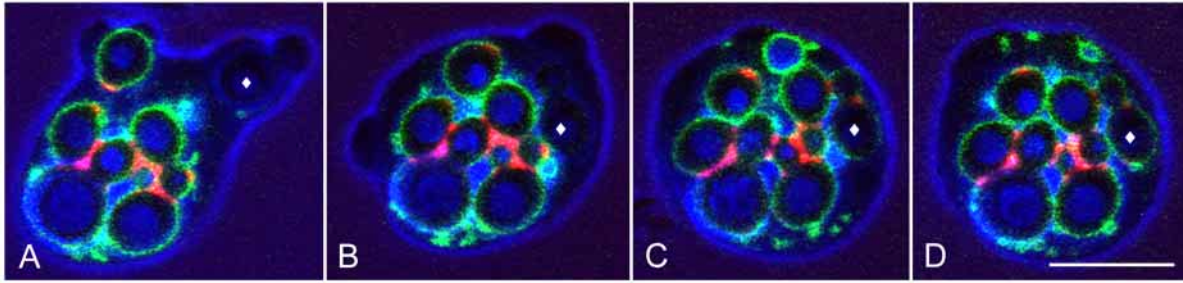
Fig. 7. Time course of VatM-GFP delivery to a new phagosome. This cell already contained several yeast particles in a multi-particle phagosome whose membrane was strongly labeled with VatM-GFP. The cell had been pre-labeled with TRITC-dextran, most of which was also localized in this large phagosomal compartment. The paucity of free endosomes correlated with slow delivery of VatM-GFP to the new phagosome. (A) Uptake of the new yeast particle; (B) 3 minutes and 15 seconds after uptake; (C) 6 minutes and 20 seconds after uptake; (D) 9 minutes after uptake. In C and D, TRITC-dextran is visible at the bud neck of the new phagosome and also at a point of contact between the new phagosome and the pre-existing phagosomal compartment, suggesting that fusion has occurred. Bar, 10 μm. (These frames are taken from Movie 2.)

lumen of the phagosome is easier to detect in such cells than in unbudded yeast, where the marker spreads out in a uniform thin layer under the phagosome membrane (not shown).

The rapidity with which the fluorescence signal from VatM-GFP in the membrane of a new phagosome reaches an intensity similar to that present in 'older' phagosomal membranes seems to depend on the availability of appropriate endosomes. If the endosome pool is large, as in the cell shown in Fig. 5B-D [and the upper cell shown in Movie 2 (available at jcs.biologists.org/supplemental)], then this occurs over a period of 3 or 4 minutes after clustering of the vesicles. If the pool is small, then substantially more time is required. Two cells in the process of phagocytosing yeast particles are shown in Movie 2; the second (lower) cell is also shown in Fig. 7. These cells were preincubated in medium containing TRITC-dextran in order to label their endosomal compartments prior to the addition of yeast. When we began this recording, the upper cell was ingesting its first yeast particle; this cell contained an abundance of VatM-GFP-labeled endosomal vesicles that clustered rapidly at the membrane of the new phagosome (Movie 2). Expression of VatM-GFP, which varies in the cell population, was not high in this cell, so the endosomes were more brightly labeled with TRITC-dextran than with VatM-GFP. TRITC dextran accumulation at the neck of the budded yeast particle was evident at 3 minutes, and several red patches were visible on the phagosome membrane at 3 to 4 minutes after particle uptake. However, VatM-GFP labeling of the phagosome membrane was hazy in this weakly expressing cell.

The second cell, just below, was expressing a high level of VatM-GFP. It phagocytosed a yeast particle about two minutes after the first cell had done so (Fig. 7A). This second cell already contained several phagosomes whose membranes were strongly labeled with VatM-GFP, and the budded yeast particles within those phagosomes had bright red collars of TRITC-dextran at the bud necks. In fact, virtually all of the TRITC-dextran and VatM-GFP available in the endosomal compartments of this cell appeared to have been provided to these earlier phagosomes, which had merged to form a multi-particle compartment. Close inspection of this video sequence suggests that fusion between the new phagosome and the pre-existing compartment occurred between 5 and 6 minutes after

uptake of the new yeast particle. Starting in that interval, VatM-GFP appeared and grew steadily brighter in the membrane of the new phagosome, reaching an intensity close to that of the pre-existing phagosomes by about 9 minutes after uptake (Fig. 7D). About 6 minutes after uptake, TRITC-dextran could be observed not only at the yeast bud neck but also at the point of contact between the new phagosome and the pre-existing phagosomal compartment, indicating that membrane fusion had taken place (arrow in Movie 2; Fig. 7C,D). We conclude that the delivery of proton pumps to phagosomes occurs predominantly through fusion of pre-existing endosomes and phagosomes with the new phagosome and that this takes place within a few minutes of uptake of a yeast particle.

As is evident in Fig. 6A, Neutral Red does not stain living yeast cells. Thus, a landmark in the phagocytic pathway is the point at which a phagocytosed yeast particle becomes permeabilized, allowing Neutral Red to stain its cytoplasm. Cytoplasmic staining implies that lysosomal enzymes have been at work on the yeast particle. Fig. 8 shows an example of a yeast particle that has reached this stage of digestion. The two images were recorded 30 seconds apart. Note that VatM-
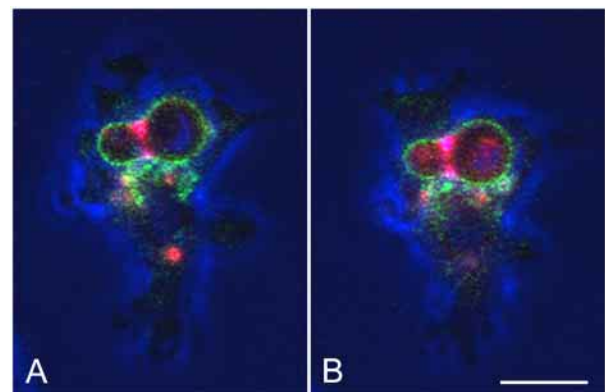

Fig. 8. Digestion of a yeast particle indicated by Neutral Red staining of the yeast cytoplasm. Neutral Red is excluded from living yeast particles but floods and stains the cytoplasm of phagocytosed yeast particles when digestion has progressed sufficiently. This transition takes place suddenly. VatM-GFP is still present in the phagosome membrane at this time. The image in B was recorded 30 seconds after the image in A. Bar, 10 μm.
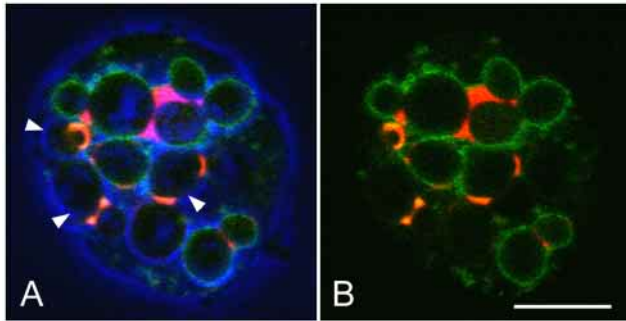
Fig. 9. Late phagosomes without membrane labeling by VatM-GFP. The membrane of the multi-particle phagosome in the upper part of this cell is labeled with VatM-GFP. TRITC-dextran has accumulated between yeast particles in this phagosome as well as at the bud necks. Below this large compartment are three phagosomes without VatM-GFP in their membranes (arrowheads); the presence of TRITC-dextran indicates that these are late phagosomes. The image in B is the same as that in A, but without the blue (phase contrast) channel. Bar, 10 μm.

GFP was still present in the phagosome membrane at the time when the yeast cytoplasm became accessible to Neutral Red.

Late phagosomes and retrieval of VatM-GFP

We found that VatM-GFP disappears from the phagosome membrane before the cell exocytoses the indigestible remnants of a yeast particle. In cell populations that had been incubated with yeast particles for more than two hours, there were many unlabeled phagosomes. If the cells had been preincubated with TRITC-dextran, the yeast particles within the VatM-GFP-deficient phagosomes had a collar of TRITC-dextran encircling the bud neck (Fig. 9, arrows), indicating that these phagosomes were not newly formed, but had previously fused with endosomal vesicles and acquired TRITC-dextran and hence also VatM-GFP. (The cell shown in Fig. 9 also contained a large multi-particle phagosome whose membrane was brightly labeled with VatM-GFP; this phagosome presumably represents an earlier stage in the pathway.)

It is also possible to capture the actual expulsion event, in which a cell exocytoses the remains of a digested yeast particle. Fig. 10 shows a cell that contained three phagosomes, each with a yeast particle. Two of the yeast particles had buds,

allowing TRITC-dextran accumulation at the bud neck to be visualized. One of the budded yeast particles resided in a phagosome whose membrane was devoid of VatM-GFP, whereas the other phagosome containing a budded yeast particle still had a GFP rim. The yeast particle from the unlabeled phagosome was expelled from the cell during the course of observation (Fig. 10C-D and Movie 3; available on-line at www.biologists.org/supplemental). The rapidity of expulsion (between one frame and the next, 5 seconds apart) is in contrast to uptake, which is more leisurely, extending over about 15 seconds (Movie 2).

Discussion

VatM-GFP as a marker for vacuolar proton pump dynamics in *Dictyostelium*

We selected VatM, the 100 kDa subunit of the *Dictyostelium* vacuolar proton pump, as our marker for localization and trafficking of the vacuolar proton pump. Our studies (Liu et al., 2002) and studies of homologous subunits in other organisms have shown that the 100 kDa V-ATPase subunit functions in the targeting and assembly of the enzyme complex, as well as in proton translocation itself (reviewed by Forgac, 2000). Using standard molecular genetic techniques, we expressed in *Dictyostelium* a fusion of VatM with GFP and monitored the behavior of the fusion protein in living cells by confocal microscopy.

We found that VatM-GFP was correctly targeted to the same *Dictyostelium* membranes in which wild-type VatM is found, namely, membranes of the contractile vacuole complex and the endolysosomal system. Furthermore, VatM-GFP appeared to be competent to direct assembly of the enzyme. That is, expression of VatM-GFP in a mutant cell line deficient in wild-type VatM (Liu et al., 2002) resulted in redistribution of VatA, the catalytic subunit of the V_1 sector, from a diffuse cytoplasmic distribution in the mutant cells to a normal location on contractile vacuole membranes in VatM-GFP-expressing cells. These results indicate that VatM-GFP is targeted to the proper endomembranes, where it serves as the locus for enzyme assembly.

The distribution of VatM-GFP within the *Dictyostelium* contractile vacuole complex was consistent with that of vacuolar proton pumps observed by other methods. Both electron microscopy of freeze-dried cells and immunostaining of fixed cells with anti-V-ATPase antibodies have shown that
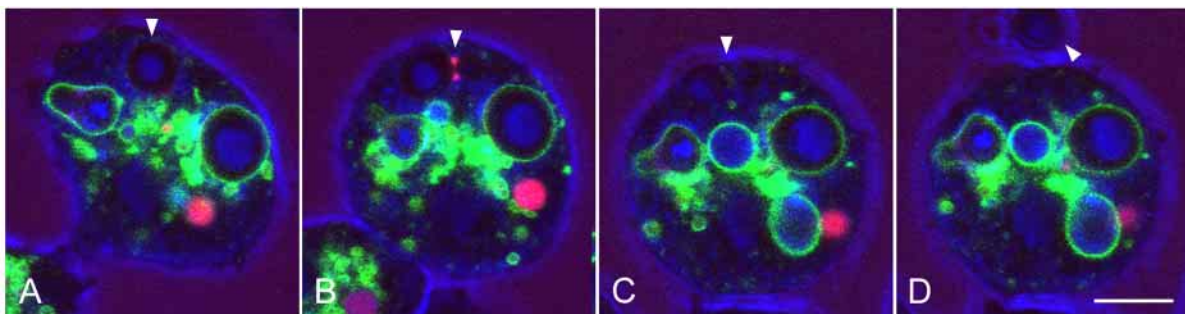

Fig. 10. Exocytosis of a digested yeast particle. (A-D) A cell containing two phagosomes with VatM-GFP-labeled membranes and a third with an unlabeled membrane (arrowheads). (A) A focal plane showing all three phagosomes; (B) a focal plane showing that the bud neck of the yeast particle in the unlabeled phagosome has a TRITC-dextran collar and is therefore a late phagosome; (C,D) two frames 5 seconds apart showing expulsion of the yeast particle from the unlabeled phagosome. Bar, 10 μm. (These frames are taken from Movie 3.)

vacuolar proton pumps are distributed throughout all membranes of the contractile vacuole system (Heuser et al., 1993; Clarke and Heuser, 1997). Likewise, as we show here, VatM-GFP brightly labeled all elements of the contractile vacuole system, both vacuolar and tubular, throughout their cycles of filling and discharge. These data also confirmed that a reversible interconversion of tubular and cisternal elements of the system occurs as fluid is accumulated and expelled, as previously inferred from observations of living cells by interference reflection microscopy and styryl dye staining (Heuser et al., 1993) and by the use of dajumin-GFP as a label for contractile vacuole membranes (Gabriel et al., 1999). In mitotic cells, where the contractile vacuole system fragments into many small vacuoles (Zhu and Clarke, 1992; Gabriel et al., 1999), these vacuoles continue to be brightly labeled with VatM-GFP and remain fully active in fluid accumulation (J.H. and M.C., unpublished). Thus, VatM-GFP in the contractile vacuole system of living cells behaves as expected for a V-ATPase marker.

Population measurements of the trafficking of vacuolar proton pumps and the evolution of endosomal pH

The presence of vacuolar proton pumps in membranes of endosomes and phagosomes from *Dictyostelium* and mammalian cells and their probable role in acidification of these organelles were first recognized by observing the effects of inhibitors and antibodies (Yamashiro et al., 1983; Padh et al., 1989; Sato and Toyama, 1994). Immunostaining revealed a rapid enrichment of V-ATPase subunits in phagosome membranes during the first 10 minutes or so after particle uptake (Pitt et al., 1992b; Temesvari et al., 1994; Nolta et al., 1994; Rebazek et al., 1997). More sophisticated analytical methods such as microsequencing (Adessi et al., 1995) and peptide mass fingerprinting (Garin et al., 2001) verified the presence of V-ATPase subunits in endosomal membranes. In *Dictyostelium,* which neutralizes late endosomes and then exocytoses the indigestible remnants of endocytosed or phagocytosed material (reviewed by Maniak, 1999), the level of V-ATPase subunits was found to drop in membranes of late endosomes (Nolta et al., 1994).

The kinetics of pH evolution along the endosomal pathway in *Dictyostelium* were defined by Satre and co-workers, who employed both ^{31}P-NMR (Brenot et al., 1992) and fluorescence spectroscopy (Aubry et al., 1993) to analyze fluid phase endocytosis. Mathematical modeling of the transit of FITC-dextran in cells incubated in nutrient medium (Aubry et al., 1997) indicated that endosomes are acidified rapidly, reaching a minimal pH value of ~5.1 about 15 minutes after uptake. During the next 40 minutes, the pH rises, stabilizing at ~pH 6.3. After a total of about 60 minutes, pseudo-first order efflux occurs. Taken together, these studies of *Dictyostelium* cell populations demonstrated that a temporal correlation exists between high levels of V-ATPase subunits in endosomal membranes and acidification of endosomal contents, and between reduced levels of the V-ATPase and subsequent reneutralization.

Single-cell observations of pH evolution and protein trafficking in *Dictyostelium*

The present study and other recent studies discussed below have employed imaging methods that allow the behavior of individual cells to be tracked. This approach provides information that the population measurements described above cannot. Microscopic observations of living cells make apparent the great heterogeneity of cell behavior, for example, with respect to the elapsed time between exposure of a cell population to a suspension of particles and the uptake of a particle by any given cell. For population measurements (biochemical, enzymatic, or spectroscopic), this heterogeneity has the effect of broadening the time interval during which a given step in a pathway appears to occur and of blurring any boundaries between steps. Thus, when dealing with asynchronous behaviors, observation of individual cells provides a much better definition of the temporal relationship between events.

Using VatM-GFP as our marker for trafficking of vacuolar proton pumps, we have found that this enzyme is brought to new phagosomes by acidic endosomal vesicles that cluster at the phagosome membrane, beginning 1 to 2 minutes after the uptake of a yeast particle. Judging from the intensity of the GFP signal, the concentration of proton pumps in the membrane of the new phagosome increases over the next few minutes. If a cell contains many VatM-GFP-positive endosomal vesicles, the fluorescence in the membrane of the new phagosome reaches a level similar to that of pre-existing phagosomes by about 4 minutes after particle uptake. Proton pumps can also be acquired through fusion with existing phagosomes.

These data indicate that in *Dictyostelium* the proton pumps are recycled in the endosomal pathway and that most of the pumps delivered to a new endosome are derived from endosomes that had already progressed to a later stage of the pathway. Of course, the proton pumps must initially be fed into the pathway through Golgi-derived vesicles or tubular extensions of the Golgi apparatus, but the contribution of de novo synthesized pumps seems to be minor relative to recycled ones, and it could not be detected by our methods.

Although the same isoform of VatM populates membranes of endosomes and of the contractile vacuole complex, we saw no evidence for a direct transfer of proton pumps from contractile vacuole membranes to phagosomes. Occasionally yeast-containing phagosomes and elements of the contractile vacuole system abutted each other in a cell, but this seemed to be a random and transient situation. In addition, VatM-GFP labeling of the contractile vacuole complex remained very bright even in cells that had taken up several yeast particles, as is evident in Movie 3 and also in Fig. 7C and D, which shows a contractile vacuole discharge.

A mixture of FITC and TRITC dextrans has been used to monitor pH changes during endosomal transit in *Dictyostelium* (Jenne et al., 1998; Maniak, 1999). Since FITC fluorescence is quenched at low pH, whereas TRITC fluorescence is insensitive to pH, the differential pH sensitivity of the two probes results in color changes from yellow-orange (extracellular and newly ingested) to red (acidified) to yellow-orange (neutralized) as the dextran mixture proceeds along the endosomal pathway. This technique is suitable not only for spectroscopic measurements but also for the visualization of pH changes in individual cells by confocal microscopy. Consistent with our results, Maniak was able to detect the rapid acidification of a macropinosome 50 to 60 seconds after uptake

(Maniak, 2001). He also detected, at an indeterminate time after uptake, the neutralization of a phagosome over a period of 2 minutes, followed by its exocytosis 16 minutes later (Maniak, 1999).

Since most aspects of macropinosome uptake are similar to phagocytosis, including the changes in membrane composition (reviewed by Cardelli, 2001) and the clustering of vesicles at the endosomal membrane during the first few minutes after uptake (Schneider et al., 2000), we expect that the delivery of proton pumps to macropinosomes and phagosomes proceeds in a similar manner, namely, by fusion with pre-existing acidic endosomes. However, fusion of a single acidic endosome, contributing both proton pumps and acidic solutes, may be sufficient to produce a large impact on the pH of a new macropinosome, whereas fusion of multiple endosomes may be needed to produce a comparable effect on a large phagosome. Further studies in individual cells will be needed to determine the relationship between endosome volume, the time course of acidification, and the time required for proton pump density to reach maximal levels in an endosomal membrane.

Fusions of cytoskeletal and signal-transduction proteins with GFP have allowed several steps in phagosome formation and maturation to be visualized in living *Dictyostelium* cells (reviewed by Maniak, 1999; Rupper and Cardelli, 2001). Particles such as yeast, bacteria and latex beads are taken up in individual phagosomes through an actin- and G-protein-dependent process (Peracino et al., 1997). Actin and actin-binding proteins dissociate from the new phagosome within about one minute of internalization (Maniak et al., 1995; Hacker et al., 1997; Rupper et al., 2001a). Rab7, which may regulate homotypic fusion events between early endosomes (Laurent et al., 1998), labels the membrane of new phagosomes within 60 seconds of internalization, as monitored using a GFP-Rab7 fusion protein (Rupper et al., 2001a). Golvesin, a membrane protein, is delivered to the membrane of new endosomes within 4-5 minutes of uptake. Like VatM-GFP, it is brought by vesicles that cluster at the endosomal membrane (Schneider et al., 2000). Lysosomal enzymes that contain N-acetylglucosamine-1-phosphate residues (e.g., cysteine proteinases) are delivered to phagosomes within 3 minutes of ingestion, as determined by antibody staining of fixed cells (Souza et al., 1997). Hence, the timing of the delivery of Rab 7, golvesin, and this class of lysosomal enzymes is similar to what we have observed for VatM-GFP. A clear implication is that several of these proteins may be delivered as components of the same vesicle.

In analyzing trafficking behavior, the nature of the phagocytosed particle must also be considered, as demonstrated previously (Souza et al., 1997). These workers found that in cells fed bacteria, two classes of lysosomal enzymes were delivered to phagosomes with different time courses. The first class (those modified with N-acetylglucosamine-1-phosphate residues) was found in endosomes after about 3 minutes, whereas the second (those modified with mannose-6-phosphate residues; e.g., α-mannosidase and β-glucosidase) was found in endosomes after about 15 minutes. Importantly, this temporal separation between the delivery of the two classes of lysosomal enzymes was not observed for phagosomes containing latex beads (Souza et al., 1997; Rupper et al., 2001a). Similarly, the V-ATPase was not retrieved from phagosome membranes of

cells fed large polystyrene or latex beads, even after 300 minutes of chase (Rezabek et al., 1997). Such observations suggest that *Dictyostelium* amoebae may utilize different trafficking pathways depending on the chemistry of the phagocytosed particle, as has been reported for macrophages (Oh and Swanson, 1996).

Later stages of phagosome processing in *Dictyostelium*

The transit time of phagocytosed particles is longer than for endocytosed fluid. We have observed neutralization of yeast-containing phagosomes ~75 minutes after uptake (data not shown), and Cardelli's group has reported neutralization of bacteria-containing phagosomes ~60 minutes after uptake (Rupper et al., 2001b; Rupper and Cardelli, 2001). The processing of yeast and bacteria is therefore likely to be similar and delayed relative to the neutralization of macropinosomes, which begins about 45 minutes after fluid uptake (Aubry et al., 1993; Maniak et al., 2001). Rupper et al. reported that, late in the pathway, neutralized phagosomes fuse to form multi-particle compartments, which they termed 'spacious' phagosomes (Rupper et al., 2001b). We too have observed multi-particle phagosomes, but, as shown in Movie 2 and Fig. 7, these can be formed by very early fusion events and may even be instrumental in the delivery of proton pumps to new phagosomes. In our study, multi-particle phagosomes (Figs 7 and 9) were VatM-GFP-positive and not 'spacious' but had a membrane that fit snugly about the yeast particles. Furthermore, late phagosomes, identified by the presence of TRITC-dextran and the lack of proton pumps, typically contained single yeast particles (Figs 9 and 10).

We have occasionally observed phagosomes that contained a large volume of fluid around the yeast particle, but these were very rare. In one case, a VatM-GFP-labeled phagosome with a single yeast particle expanded from a snug fit to a roomy, fluid-filled compartment in less than 10 seconds, suggesting that the change occurred through fusion with a large endosome (data not shown). In another case, a roomy multi-particle phagosome containing three yeast particles was converted to a tight fit and then became separated into three vesicles each with a single yeast particle, two of which were consecutively exocytosed (A. Benjak and G.G., unpublished). Thus, in our studies, roomy phagosomes were not confined to a particular stage of the endocytic pathway, and their rarity suggested that they represented an infrequent or highly transient state.

Our data indicate that exocytosis of the indigestible remnants of a yeast particle occurs after retrieval of proton pumps from the phagosome membrane. We anticipate that the retrieval of proton pumps will prove to be linked to the rise in lumenal pH that occurs in late endosomes and phagosomes, although this has not been explicitly demonstrated. As noted above, Maniak reported exocytosis of a yeast particle 16 minutes after the phagosome had been neutralized (Maniak, 1999), while Rupper et al. reported that spacious phagosomes still persisted more than an hour after neutralization had been observed (Rupper et al., 2001b). Hence, experimental conditions may have a profound impact on this aspect of cell behavior. In future studies, it will be important to monitor simultaneously the retrieval of VatM-GFP and the timing of neutralization and exocytosis.

Relationship to endosome-phagosome interactions in mammalian cells

There are many common features between the endocytic pathways in *Dictyostelium* and in mammalian cells, but in some respects our data differ from those reported for mammalian cells. A common theme is the interactions between endosomes and phagosomes. In J-774 macrophages, Mayorga et al. showed that within 10 minutes of phagocytosis, both endosomes and lysosomes fused with phagosomes (Mayorga et al., 1991). This same group reported that radiolabeled protein originally associated with phagocytosed particles could be found 18 minutes later in a non-phagosome vesicle population that displayed some endosomal characteristics (Pitt et al., 1992a). Desjardins et al. reported that the fluid content of latex-bead-containing phagosomes and late endocytic organelles became completely intermixed within 60-90 minutes after the uptake of the beads (Desjardins et al., 1994), whereas the transfer of a late endosomal membrane protein (lamp-2) required about 6 hours. Using video microscopy, these workers detected multiple transient interactions between late endocytic organelles (pre-loaded with gold particles) and newly formed latex-bead-containing phagosomes. Similarly, Jahraus et al. demonstrated that there was retrograde traffic of contents between lysosomes and late endosomes (Jahraus, 1994). Together, these observations suggested that phagosomes acquire markers from endocytic organelles through successive interactions in a gradual and regulated process.

On the basis of such data, it has been proposed that the interaction between endocytic organelles and phagosomes is not necessarily a complete fusion but rather a partial exchange of fluid and membrane proteins (reviewed by Tjelle et al., 2000). This 'kiss and run' hypothesis (Desjardins, 1995) has been supported by the finding that large and small endocytosed molecules appear in phagosomes with different kinetics (Wang and Goren, 1987; Desjardins et al., 1997) and that phagosomes do not acquire endocytic solutes and membrane proteins simultaneously (Desjardins et al., 1994).

The endosome-phagosome interactions in our study were recorded at 5 second intervals and were taken from single focal planes. This temporal and spatial resolution is not adequate to allow us to track individual endosomal vesicles and determine with certainty that a particular endosome-phagosome interaction resulted in complete fusion. However, it is clear that endosomal vesicles clustered at the membrane of a new phagosome during the first few minutes after uptake and that, within the limits of our resolution, VatM-GFP and the TRITC-dextran content of the endosomes were delivered to the new phagosome with the same time course. Thus, the simplest explanation for our results is that endosomal vesicles containing TRITC-dextran in their lumen and VatM-GFP in their membrane, fused completely with the phagosome. We speculate that vesicles with different lumenal content and membrane composition may be capable of fusing with phagosomes at specific stages of their maturation.

The use of multiple probes will be required to determine whether other proteins are delivered to phagosomes as components of the same vesicle population as VatM-GFP. The recent demonstration that a fusion of the cysteine proteinase cathepsin B with GFP is correctly targeted to endosomes (Lincke et al., 2001) opens the way for the simultaneous tracking of pairs of proteins labeled with color-shifted GFP variants. These methods should make it possible to monitor the delivery and retrieval of vacuolar proton pumps in direct comparison with the delivery of lysosomal enzymes, thereby providing new insights into the mechanisms of endo-lysosomal trafficking.

References

Adessi, C., Chapel, A., Vincon, A., Rabilloud, T., Klein, G., Satre, M. and Garin, J. (1995). Identification of major proteins associated with *Dictyostelium discoideum* endocytic vesicles. *J. Cell Sci.* **108**, 3331-3337.

Aubry, L., Klein, G., Martiel, J.-L. and Satre, M. (1993). Kinetics of endosomal pH evolution in *Dictyostelium discoideum* amoebae. Study by fluorescence spectroscopy. *J. Cell Sci.* **105**, 861-866.

Aubry, L., Klein, G., Martiel, J.-L. and Satre, M. (1997). Fluid-phase endocytosis in the amoebae of the cellular slime mould *Dictyostelium discoideum*: Mathematical modeling of kinetics and pH evolution. *J. Theor. Biol.* **184**, 89-98.

Brénot, F., Aubry, L., Martin, J. B., Satre, M. and Klein, G. (1992). Kinetics of endosomal acidification in *Dictyostelium discoideum* amoebae. ^{31}P-NMR evidence for a very acidic early endosomal compartment. *Biochimie* **74**, 883-895.

Bush, J., Temesvari, L., Rodriguez-Paris, J., Buczynski, G. and Cardelli, J. (1996). A role for a Rab4-like GTPase in endocytosis and in regulation of contractile vacuole structure and function in *Dictyostelium discoideum*. *Mol. Biol. Cell* **7**, 1623-1638.

Cardelli, J. (2001). Phagocytosis and macropinocytosis in *Dictyostelium*: Phosphoinositide-based processes, biochemically distinct. *Traffic* **2**, 311-320.

Clarke, M. and Heuser, J. (1997). Water and ion transport. In *Dictyostelium-A Model System for Cell and Developmental Biology* (ed. Y. Maeda, K. Inouye and I. Takeuchi), pp. 75-91. Tokyo: Universal Academic Press Inc.

Clarke, M., Bazari, W. L. and Kayman, S. C. (1980). Isolation and properties of calmodulin from *Dictyostelium discoideum*. *J. Bact.* **141**, 397-400.

Clarke, M., Kayman, S. C. and Riley, K. (1987). Density-dependent induction of discoidin-I synthesis in exponentially growing cells of *Dictyostelium discoideum*. *Differentiation* **34**, 79-87.

Cross, R. L. and Duncan, T. M. (1996). Subunit rotation in F_1F_0-ATPases as a means of coupling proton transport through F_0 to the binding changes in F_1. *J. Bioenerg. Biomemb.* **28**, 403-408.

Desjardins, M. (1995). Biogenesis of phagolysosomes: The "kiss and run" hypothesis. *Trends Cell Biol.* **5**, 183-186.

Desjardins, M., Huber, L. A., Parton, R. G. and Griffiths, G. (1994). Biogenesis of phagolysosomes proceeds through a sequential series of interactions with the endocytic apparatus. *J. Cell Biol.* **124**, 677-688.

Desjardins, M., Nzala, N. N., Corsini, R. and Rondeau, C. (1997). Maturation of phagosomes is accompanied by changes in their fusion properties and size-selective acquisition of solute materials from endosomes. *J. Cell Sci.* **110**, 2303-2314.

Fok, A. K., Clarke, M., Ma, L. and Allen, R. D. (1993). Vacuolar H+-ATPase of *Dictyostelium discoideum*. A monoclonal antibody study. *J. Cell Sci.* **106**, 1103-1113.

Forgac, M. (2000). Structure, mechanisms and regulation of the clathrin-coated vesicle and yeast vacuolar H+-ATPases. *J. Exp. Biol.* **203**, 71-80.

Gabriel, D., Hacker, U., Köhler, J., Muller-Taubenberger, A., Schwartz, J.-M., Westphal, M. and Gerisch, G. (1999). The contractile vacuole network of *Dictyostelium* as a distinct organelle: its dynamics visualized by a GFP marker protein. *J. Cell Sci.* **112**, 3995-4005.

Garin, J., Diez, R., Kieffer, S., Dermine, J.-F., Duclos, S., Gagnon, E., Sadoul, R., Rondeau, C. and Desjardins, M. (2001). The phagosome proteome: Insight into phagosome functions. *J. Cell Biol.* **152**, 165-180.

Hacker, U., Albrecht, R. and Maniak, M. (1997). Fluid-phase uptake by macropinocytosis in *Dictyostelium. J. Cell Sci.* **110**, 105-112.

Heuser, J., Zhu, Q. and Clarke, M. (1993). Proton pumps populate the contractile vacuoles of *Dictyostelium* amoebae. *J. Cell Biol.* **121**, 1311-1327.

Jackson, D. D. and Stevens, T. H. (1997). *VMA12* encodes a yeast endoplasmic reticulum protein required for vacuolar H+-ATPase assembly. *J. Biol. Chem.* **272**, 25928-25934.

Jahraus, A., Storrie, B., Griffiths, G. and Desjardins, M. (1994). Evidence for retrograde traffic between terminal lysosomes and the prelysosomal/late endosome compartment. *J. Cell Sci.* **107**, 145-157.

Jenne, N., Raunchenberger, R., Hacker, U., Kast, T. and Maniak, M. (1998). Targeted gene disruption reveals a role for vacuolin B in the late endocytic pathway and exocytosis. *J. Cell Sci.* **111**, 61-70.

Junge, W., Sabbert, D. and Engelbrecht, S. (1996). Rotary catalysis: Real time recording of intersubunit rotation. *Ber. Bunsenges. Phys. Chem.* **100**, 2014-2019.

Kane, P. M. (1995). Disassembly and reassembly of the yeast vacuolar H+-ATPase in vivo. *J. Biol. Chem.* **270**, 17025-17032.

Landolt-Marticorena, C., Kahr, W. H., Zawarinski, P., Correa, J. and Manolson, M. F. (1999). Substrate and inhibitor-induced conformational changes in the yeast V-ATPase provide evidence for communication between the catalytic and proton-translocating sectors. *J. Biol. Chem.* **274**, 26057-26064.

Landolt-Marticorena, C., Williams, K. M., Correa, J., Chen, W. and Manolson, M. F. (2000). Evidence that the NH2 Terminus of Vph1p, an integral subunit of the V0 sector of the yeast V-ATPase, interacts directly with the Vma1p and Vma13p subunits of the V1 sector. *J. Biol. Chem.* **275**, 15449-15457.

Laurent, O., Bruckert, F., Adessi, C. and Satre, M. (1998). *In vitro* reconstituted *Dictyostelium discoideum* early endosome fusion is regulated by Rab7 but proceeds in the absence of ATP-MG2+ from the bulk solution. *J. Biol. Chem.* **273**, 793-799.

Leng, X.-H., Manolson, M. F., Liu, Q. and Forgac, M. (1996). Site-directed mutagenesis of the 100-kDa subunit (Vph1p) of the yeast vacuolar (H+)-ATPase. *J. Biol. Chem.* **271**, 22487-22493.

Leng, X.-H., Manolson, M. F. and Forgac, M. (1998). Function of the COOH-terminal domain of Vph1p in activity and assembly of the yeast VpATPase. *J. Biol. Chem.* **273**, 6717-6723.

Leng, X.-H., Nishi, T. and Forgac, M. (1999). Transmenbrane topography of the 100-kDa a subunit (Vph1p) of the yeast vacuolar proton-translocation ATPase. *J. Biol. Chem.* **274**, 14655-14661.

Lincke, M., Herzog, V. and Brix, K. (2001). Cathepsin-B-GFP illuminates secretion of mature lysosomal enzymes from thyrocytes. *Mol. Biol. Cell* **12S**, 344a.

Liu, T. and Clarke, M. (1996). The vacuolar proton pump of *Dictyostelium discoideum*: molecular cloning and analysis of the 100-kDa subunit. *J. Cell Sci.* **109**, 1041-1051.

Liu, T., Mirschberger, C., Chooback, L., Arana, Q., Dal Sacco, Z., MacWilliams, H. and Clarke, M. (2002). Altered expression of the 100-kDa subunit of the *Dictyostelium* vacuolar proton pump impairs enzyme assembly, endocytic function, and cytosolic pH regulation. *J. Cell Sci.* **115**, 1907-1918.

Loomis, W. F. (1975). *Dictyostelium discoideum. A developmental system.* New York: Academic Press.

Maniak, M. (1999). Green fluoresecnt protein in the visualization of particle uptake and fluid-phase endocytosis. *Meth. Enzymol.* **302**, 43-50.

Maniak, M. (2001). Fluid-phase uptake and transit in axenic *Dictyostelium* cells. *Biochim. Biophys. Acta* **1525**, 197-204.

Maniak, M., Rauchenberger, R. Albrecht, R., Murphy, J. and Gerisch, G. (1995). Coronin involved in phagocytosis: dynamics of particle-induced relocalization visualized by a green fluorescent protein tag. *Cell* **83**, 915-924.

Manolson, M. F., Proteau, D., Preston, R. A., Stenbit, A., Roberts, B. T., Hoyt, M. A., Preuss, D., Mulholland, J., Botstein, D. and Jones, E. W. (1992). The *VPH1* gene encodes a 95-kDa integral membrane polypeptide required for in vivo assembly and activity of the yeast vacuolar H+-ATPase. *J. Biol. Chem.* **267**, 14294-14303.

Manolson, M. F., Wu, B., Proteau, D., Taillon, B. E., Roberts, B. T., Hoyt, M. A. and Jones, E. W. (1994). *STV1* gene encodes functional homologue of 95-kDa yeast vacuolar H+-ATPase subunit Vph1p. *J. Biol. Chem.* **269**, 14064-14074.

Manstein, D. J., Schuster, H.-P., Morandini, P. and Hunt, D. M. (1995). Cloning vectors for the production of proteins in *Dictyostelium discoideum. Gene* **162**, 129-134.

Mattsson, J. P., Li, X., Peng, S. B., Nilsson, F., Anderson, P., Lundberg, L. G., Stone, D. K. and Keeling, D. J. (2000). Properties of three isoforms of the 116-kDa subunit of vacuolar H+-ATPase from a single vertebrate species. Cloning, gene expression, and protein characterization of functionally distinct isoforms in *Gallus gallus. Eur. J. Biochem.* **267**, 4115-4126.

Mayorga, L. S., Bertini, F. and Stahl, P. D. (1991). Fusion of newly formed phagosome with endosomes in intact cells and in a cell-free system. *J. Biol. Chem.* **266**, 6511-6517.

Nelson, N. and Harvey, W. R. (1999). Vacuolar and plasma membrane V-ATPases. *Physiol. Rev.* **79**, 361-385.

Nishi, T. and Forgac, M. (2000). Molecular cloning and expression of three isoforms of the 100-kDa a subunit of the mouse vacuolar proton-translocating ATPase. *J. Biol. Chem.* **275**, 6824-6830.

Noji, H., Yasuda, R., Yoshida, M. and Kazuhiko, K. (1997). Direct observation of the rotation of the F1-ATPase. *Nature* **386**, 299-302.

Nolta, K. V., Rodriguez-Paris, J. M. and Steck, T. L. (1994). Analysis of successive endocytic compartments isolated from *Dictyostelium discoideum* by magnetic fractionation. *Biochim. Biophys. Acta* **1224**, 237-246.

Oh, Y.-K. and Swanson, J. A. (1996). Different fates of phagocytosed particles after delivery into macrophage lysosomes. *J. Cell Biol.* **132**, 585-593.

O'Halloran, T. J. and Anderson, R. G. (1992). Clathrin heavy chain is required for pinocytosis, the presence of large vacuoles, and development in *Dictyostelium. J. Cell Biol.* **118**, 371-377.

Oka, T., Toyomura, T., Honjo, K., Wada, Y. and Futai, M. (2001). Four subunit a isoforms of *Caenorhabditis elegans* vacuolar H+ ATPase: Cell-specific expression during development. *J. Biol. Chem.* **276**, 33079-33085.

Padh, H., Lavasa, M. and Steck, T. L. (1989). Prelysosomal acidic vacuoles in *Dictyostelium discoideum. J. Cell Biol.* **108**, 865-874.

Peracino, B., Borleis, J., Jin, T., Westphal, M., Schwartz, J. M., Wu, L., Bracco, E., Gerisch, G., Devreotes, P. and Bozzaro, S. (1998). G protein β subunit-null mutants are impaired in phagocytosis and chemotaxis due to inappropriate regulation of the actin cytoskeleton. *J. Cell Biol.* **141**, 1529-1537.

Pitt, A., Mayorga, L. S., Schwarz, A. L. and Stahl, P. D. (1992a). Transport of phagosomal components to an endosomal compartment. *J. Biol. Chem.* **267**, 126-132.

Pitt, A., Mayorga, L. S., Stahl, P. D. and Schwartz, A. L. (1992b). Alterations in the protein composition of maturing phagosomes. *J. Clin. Invest.* **90**, 1978-1983.

Rathi, A., Kayman, S. C. and Clarke, M. (1991). Induction of gene expression in *Dictyostelium* by prestarvation factor, a factor secreted by growing cells. *Dev. Genet.* **12**, 82-87.

Rezabek, B. L., Rodriguez-Paris, J. M., Cardelli, J. A. and Chia, C. P. (1997). Phagosomal proteins of *Dictyostelium discoideum. J. Euk. Microbiol.* **44**, 284-292.

Rodriguez-Paris, J. M., Nolta, K. V. and Steck, T. L. (1993). Characterization of lysosomes isolated from *Dictyostelium discoideum* by magnetic fractionation. *J. Biol. Chem.* **268**, 9110-9116.

Rose, M. D., Winston, F. and Hieter, P. (1990). *Methods in Yeast Genetics: A Laboratory Course Manual.* Cold Spring Harbor, New York: Cold Spring Harbor Laboratory Press.

Rupper, A. and Cardelli, J. (2001). Regulation of phagocytosis and endo-phagosomal trafficking pathways in *Dictyostelium discoideum. Biochim. Biophys. Acta* **1525**, 205-216.

Rupper, A., Grove, B. and Cardelli, J. (2001a). Rab7 regulates phagosome maturation in *Dictyostelium. J. Cell Sci.* **114**, 2449-2460.

Rupper, A. C., Rodriguez-Paris, J. M., Grove, B. D. and Cardelli, J. A. (2001b). p110-related PI3-kinases regulate phagosome-phagosome fusion and phagosomal pH through a PKB/Akt dependent pathway in *Dictyostelium. J. Cell Sci.* **114**, 1283-1295.

Ruscetti, T., Cardelli, J. A., Niswonger, M. L. and O'Halloran, T. J. (1994). Clathrin heavy chain functions in sorting and secretion of lysosomal enzymes in *Dictyostelium discoideum. J. Cell Biol.* **126**, 343-352.

Sato, S. B. and Toyama, S. (1994). Interference with the endosomal acidification by a monoclonal antibody directed toward the 116(100)-kD subunit of the vacuolar proton pump. *J. Cell Biol.* **127**, 39-53.

Satre, M., Martin, J.-B. and Klein, G. (1989). Methyl phosphonate as a 31P NMR probe for intracellular pH measurements in *D. discoideum. Biochimie* **71**, 941-948.

Schneider, N., Schwartz, J.-M., Koehler, J., Becker, M., Schwarz, H. and Gerisch, G. (2000). Golvesin-GFP functions as distinct markers for Golgi and post-Golgi vesicles in *Dictyostelium. Biol. Cell* **92**, 485-511.

Souza, G. M., Mehta, D. P., Lammertz, M., Rodriguez-Paris, J., Wu, R., Cardelli, J. A. and Freeze, H. H. (1997). *Dictyostelium* lysosomal proteins with different sugar modifications sort to functionally distinct compartments. *J. Cell Sci.* **110**, 2239-2248.

Sumner, J. P., Dow, J. A. T., Earley, F. G. P., Klein, U., Jager, D. and Wieczorek, H. (1995). Regulation of plasma membrane V-ATPase activity by dissociation of peripheral subunits. *J. Biol. Chem*. **270**, 5649-5653.

Temesvari, L., Rodriguez-Paris, J., Bush, J., Steck, T. L. and Cardelli, J. (1994). Characterization of lysosomal membrane proteins of *Dictyostelium discoideum*. *J. Biol. Chem.* **269**, 25719-25727.

Tjelle, T. E., Lovdal, T. and Berg, T. (2000). Phagosome dynamics and function. *BioEssays* **22**, 255-263.

Wang, Y. L. and Goren, M. B. (1987). Differential and sequential delivery of fluorescent lysosomal probes into phagosomes in mouse peritoneal macrophages. *J. Cell Biol.* **104**, 1749-1754.

Wieczorek, H., Brown, D., Grinstein, S., Ehrenfeld, J. and Harvey, W. R. (1999). Animal plasma membrane energization by proton-motive V-ATPases. *BioEssays* **22**, 37-48.

Yamashiro, D. J., Fluss, S. R. and Maxfield, F. R. (1983). Acidification of endocytic vesicles by an ATP-dependent proton pump. *J. Cell Biol.* **97**, 929-934.

Yumura, S., Mori, H. and Fukui, Y. (1984). Localization of actin and myosin for the study of amoeboid movement in *Dictyostelium* using improved immunofluorescence. *J. Cell Biol.* **99**, 894-899.

Zhu, Q. and Clarke, M. (1992). Association of calmodulin and an unconventional myosin with the contractile vacuole complex of *Dictyostelium discoideum*. *J. Cell Biol.* **118**, 347-358.